J. Phys. Chem. A **2002,** *106,* 9737−9744

First-Principles Determination of the Absolute Hydration Free Energy of the Hydroxide Ion†

Chang-Guo Zhan and David A. Dixon*

Theory, Modeling & Simulation, William R. Wiley Environmental Molecular Sciences Laboratory, Pacific Northwest National Laboratory, MS K1-83, P.O. Box 999, Richland, Washington 99352

Received: December 13, 2001; In Final Form: April 5, 2002

The absolute hydration free energy of the hydroxide ion, $\Delta G^{298}_{\mathrm{hyd}}(\mathrm{HO}^-)$, a fundamental quantity in solution chemistry, has "experimental" values ranging from −90.6 to −110.0 kcal/mol. We report a first-principles determination of $\Delta G^{298}_{\mathrm{hyd}}(\mathrm{HO}^-)$ by using a reliable computational protocol of high-level first-principles supermolecule-continuum calculations, the same approach recently used to determine the absolute hydration free energy of the proton. In the supermolecule-continuum approach, part of the solvent surrounding the solute is treated quantum mechanically, and the remaining bulk solvent is approximated by a dielectric continuum medium accounted for by a recently developed self-consistent reaction field model known as surface and volume polarization for electrostatic interaction (SVPE) or the fully polarizable continuum model (FPCM). With this approach, the calculated results can systematically be improved by increasing the number of quantum mechanically treated solvent molecules, and $\Delta G^{298}_{\mathrm{hyd}}(\mathrm{HO}^-)$ is accurately predicted to be −104.5 kcal/mol. The $\Delta G^{298}_{\mathrm{hyd}}(\mathrm{HO}^-)$ value of −104.5 kcal/mol, combined with our previously determined $\Delta G^{298}_{\mathrm{hyd}}(\mathrm{H}^+)$ value of −262.4 kcal/mol, allows the prediction of the sum of absolute hydration free energies of the proton and hydroxide to be −366.9 kcal/mol, in excellent agreement with the well-established experimental thermodynamic value of −366.6 ± 0.1 kcal/mol.

Introduction

Ionic hydration plays a vital role in aqueous chemical and biological systems,[1−19] and for thermodynamic analyses, it is key to have established the absolute hydration (Gibbs) free energies of ions. Unfortunately, the absolute solvation free energy of a single ion is very difficult to determine by experiment because any stable, macroscopic solution contains equal amounts of positive and negative charge.[1,2] Without using additional approximations or models, an experiment can only be performed to determine the sum of hydration free energies of a pair of oppositely charged ions, such as $\mathrm{H}^+ + \mathrm{HO}^-$, $\mathrm{Li}^+ + \mathrm{HO}^-$, $\mathrm{Na}^+ + \mathrm{HO}^-$, $\mathrm{H}^+ + \mathrm{F}^-$, $\mathrm{Li}^+ + \mathrm{F}^-$, $\mathrm{Na}^+ + \mathrm{F}^-$, etc. It has not yet been possible to isolate one type of ion and measure its absolute hydration free energy. Hence, direct experimental data for different pairs of ions can provide information only for the relative magnitudes of the ionic hydration free energies.[20,21] Thus, it is not surprising to find that the reported "experimental" absolute hydration free energy of the proton (H^+) has a wide range from −252.6 to −264.1 kcal/mol[22a] and that of the hydroxide ion (HO^-) has an even wider range from −90.6[22b] to −110.0 kcal/mol.[22c] It is, therefore, critically important to develop reliable first-principles computational protocols for the accurate determination of the absolute hydration free energies of ions.

To predict the absolute hydration free energy of an ion, $\Delta G^{298}_{\mathrm{hyd}}(\mathrm{M}^q)$, from first principles, the conceptually simplest approach based on ab initio electronic structure theory is to converge the free energy of reaction 1 by simply increasing n until the free energy does not change on addition of successive waters:[21,23]

$$\mathrm{M}^q(\mathrm{gas}) + (\mathrm{H_2O})_n(\mathrm{gas}) \rightarrow \mathrm{M}^q(\mathrm{H_2O})_n(\mathrm{gas}) \qquad (1)$$

For large enough n, the cluster will approach the liquid. The free energy of reaction 1 converged to $n \rightarrow \infty$ is the desired absolute hydration free energy of an ion, M^q, with a net charge of q. However, the free energy of reaction 1 is slowly convergent because the bulk solvent (water) effects are dominated by long-range electrostatic interactions. High-level ab initio electronic structure calculations including even modest numbers of solvent molecules are impractical computationally.[24] We therefore have to consider alternative approaches that can practically account for the bulk solvent effects.

A computationally simpler approach is to consider an ion (as a solute) existing in an isotropic homogeneous continuous dielectric medium which can be polarized by the solute leading to a reaction field that in turn polarizes the solute itself.[25a] This approach requires that an implicit solute−solvent interaction potential, the solvent polarization potential, be included in the solute Hamiltonian. This electronic structure approach including solvation is known as the self-consistent reaction field (SCRF) theory.[26] It has been well-established that the pure continuum description of solvation is reasonable for bulk solvent effects but may not be reliable enough to treat the effects of the solvent molecules within the first solvation shell, particularly those having strong hydrogen bonds with the solute.[26d,27] This is because the continuum model itself completely ignores the solvent structure and, therefore, does not account for some important effects because of specific solute−solvent interac-

---

† Part of the special issue "Jack Beauchamp Festschrift".

* To whom correspondence should be addressed.

10.1021/jp014533l CCC: $22.00 © 2002 American Chemical Society
Published on Web 06/04/2002

tions.[27] As a result, whereas the continuum model can satisfactorily describe the dominant long-range electrostatic interactions and associated inductive interactions between solute and solvent, there are also other nonelectrostatic interactions (such as cavitation, dispersion, and Pauli repulsion) that are short-range, usually caused by the specific solute−solvent interactions, such as hydrogen bonding, within the first solvation shell.[26d] Nevertheless, in principle, the SCRF results can be improved by coupling with a supermolecule approach that includes the solute and some solvent molecules interacting with the solute so that the short-range nonelectrostatic interactions between the solute and the first-solvation-shell solvent molecules are fully included in the SCRF electronic structure calculation.[27] The overall nonelectrostatic interaction between the explicit solvent water molecules in the hydrated ion, $M^q(H_2O)_n$, and the bulk solvent should be similar to that between the corresponding water cluster, $(H_2O)_n$, and the bulk solvent, because they are all due to water−water interactions. The difference should disappear for the large n limit. Such an SCRF calculation on a supermolecule is known as the hybrid supermolecule-continuum approach. The physical meaning of such a hybrid supermolecule-continuum approach, i.e., performing an SCRF calculation on the supermolecular solute, is that the part of the solvent surrounding the solute (usually the first solvation shell) is treated quantum mechanically and the remaining bulk solvent is still approximated as the dielectric continuum medium.[27] Obviously, the more solvent molecules that are treated quantum mechanically, the better the calculated results; as noted above, the improvement on increasing the number of solvent molecules in the supermolecular solute will systematically approach the limit for large n. Thus, the hydration free energy of an ion is the free energy of reaction 2, $\Delta G_{\text{hyd}}[M^q,n]$, converged to $n \rightarrow \infty$:

$$M^q(\text{gas}) + (H_2O)_n(\text{aq}) \rightarrow M^q(H_2O)_n(\text{aq}) \tag{2}$$

With increasing n, the electronic structure calculations with the hybrid supermolecule-continuum approach for reaction 2 are expected to converge much faster than the corresponding calculations for reaction 1.

Most recent computational studies[21,22a,23,28] on the determination of the absolute hydration free energies of ions are based on the hybrid supermolecule-continuum approach using reaction 2 or its variants, although these hybrid calculations were performed with different SCRF procedures and at different electronic structure levels. Obviously, the SCRF procedure used in a hybrid supermolecule-continuum calculation is the primary variable in the reliability of the calculated results so long as the calculation is performed with enough explicitly considered solvent molecules and at a sufficiently high electronic structure level. Previous hybrid supermolecule-continuum calculations[21,22a,23] based on ab initio electronic structure theory have used simpler solvation models with empirical parameters or other approximations as well as relatively modest levels of electronic structure theory. Very recently, a surface and volume polarization for the electrostatic interaction (SVPE) procedure[25] has been employed for high-level supermolecule-continuum calculations for the first-principles determination of the absolute hydration free energy of the proton.[28] With gas-phase electronic structure calculations at the MP2 level including extrapolation to the complete basis set (CBS) limit combined with CCSD(T) correction terms plus the determined bulk solvent shifts, the calculated absolute hydration free energy of the proton converged to $\Delta G^{298}_{\text{hyd}}(H^+) = -262.4$ kcal/mol for $n = 4$ (the complete first solvation shell about H_3O^+ is explicitly included).[28] The high accuracy of the predicted absolute hydration free energy of the proton was confirmed by applying the same computational protocol to predict $\Delta G^{298}_{\text{hyd}}(Li^+)$ to be -125.1 kcal/mol.[28] The calculated hydration free energy difference between the free energy of solvation of a proton and the free energy of solvation of Li^+ is 137.5 kcal/mol from the latest collection of experimental data[20] and 137.0 kcal/mol from an earlier experimental compilation.[22b] The theoretical value[28] of 137.3 kcal/mol lies between the two experimental values.

On the basis of the success of the SVPE-based supermolecule-continuum calculations for the absolute hydration free energies of cations, we decided to calculate the absolute free energy of hydration of the hydroxide ion, $\Delta G^{298}_{\text{hyd}}(HO^-)$, by using the same computational approach. This allows us to examine whether the same SVPE-based computational protocol used for cations can be used for reliable predictions for anions. The hydroxide ion is of particular interest for aqueous chemistry and poses an interesting challenge because of the presence of the more diffuse negative charge. Once the absolute hydration free energy of an anion is known, one can compare the calculated sum of absolute hydration free energies of a pair of oppositely charged ions with well-established experimental data for the ion pair. Among numerous possible pairs of oppositely charged ions, we are particularly interested in the proton and hydroxide because they naturally exist, or coexist with other ions, in any aqueous solution. With an accurately determined $\Delta G^{298}_{\text{hyd}}(HO^-)$ value, together with the $\Delta G^{298}_{\text{hyd}}(H^+)$ value determined by using the same computational protocol, we are able to establish a complete first-principles thermodynamic understanding of the well-known water autoionization in aqueous solution and directly compare the theoretical prediction with the well-established experimental thermodynamic data.

Computational Methods

As in our previous calculation of $\Delta G^{298}_{\text{hyd}}(H^+)$, to calculate the free energy of reaction 2 for $\Delta G^{298}_{\text{hyd}}(HO^-)$, we need to know the Gibbs free energies of $HO^-(\text{gas})$, $(H_2O)_n(\text{aq})$, and $HO^-(H_2O)_n(\text{aq})$. For each of the two aqueous clusters $(H_2O)_n(\text{aq})$ and $HO^-(H_2O)_n(\text{aq})$, its free energy, $G[(H_2O)_n(\text{aq})]$ or $G[HO^-(H_2O)_n(\text{aq})]$, can be expressed as a sum of the free energy of the corresponding gas-phase cluster, $(H_2O)_n(\text{gas})$ or $HO^-(H_2O)_n(\text{gas})$, and the bulk solvent shift:

$$G[(H_2O)_n(\text{aq})] = G[(H_2O)_n(\text{gas})] + \Delta G_{\text{sol}}[(H_2O)_n] \tag{3}$$

$$G[HO^-(H_2O)_n(\text{aq})] = G[HO^-(H_2O)_n(\text{gas})] + \Delta G_{\text{sol}}[HO^-(H_2O)_n] \tag{4}$$

Thus, we can evaluate the hydration free energy of hydroxide ion via

$$\Delta G_{\text{hyd}}[HO^-,n] = \Delta G_{\text{gas}}[HO^-,n] + \Delta\Delta G_{\text{sol}}[HO^-,n] \tag{5}$$

where $\Delta G_{\text{gas}}[HO^-,n] = G[HO^-(H_2O)_n(\text{gas})] - G[(H_2O)_n(\text{gas})] - G[HO^-(\text{gas})]$ is the contribution of the explicitly included water molecules to the hydroxide hydration free energy, and $\Delta\Delta G_{\text{sol}}[HO^-,n] = \Delta G_{\text{sol}}[HO^-(H_2O)_n] - \Delta G_{\text{sol}}[(H_2O)_n]$ is due to the bulk solvent effects. At $T = 298$ K, $\Delta G_{\text{hyd}}[HO^-,n]$ is converged to $\Delta G^{298}_{\text{hyd}}(HO^-)$ when $n \rightarrow \infty$. To determine $\Delta G_{\text{hyd}}[HO^-,n]$ with high accuracy, both $\Delta G_{\text{gas}}[HO^-,n]$ and $\Delta\Delta G_{\text{sol}}[HO^-,n]$ must be calculated at a sufficiently high level of theory.

To calculate $\Delta G_{\text{gas}}[\text{HO}^-,n]$ and $\Delta\Delta G_{\text{sol}}[\text{HO}^-,n]$, we first need to optimize geometries of the appropriate structures at a sufficiently high level of theory. Our previous computational studies[28] on $\Delta G^{298}_{\text{hyd}}(\text{H}^+)$ indicate that geometry optimizations in the gas phase using gradient corrected density functional theory (DFT) with Becke's three-parameter hybrid exchange functional and the Lee–Yang–Parr correlation functional (B3LYP)[29] together with the 6-31++G** basis set[30] are adequate. The free energy changes calculated by using geometries optimized at higher levels (with the second-order Møller–Plesset (MP2) method and/or with larger basis sets) were nearly the same as those calculated by using the geometries optimized at the B3LYP/6-31++G** level.[28] The estimated bulk solvent effects on the optimized geometries are also negligible.[28] Hence, the geometries of HO^-, $(\text{H}_2\text{O})_n$, and $\text{HO}^-(\text{H}_2\text{O})_n$ optimized in the gas phase at the B3LYP/6-31++G** level can be used for the free energy of solvation calculations. The DFT geometry optimizations were followed by analytical second-derivative calculations to ensure that the optimized geometries are minima on the potential energy hypersurface (all real frequencies) and to evaluate the thermal and vibrational corrections to the Gibbs free energies (at 298 K and 1 atm).[31] We considered $n = 4$, 8, 12, and 16 with $n = 4$ for the complete first solvation shell and $n > 4$ for inclusion of water molecules beyond the first solvation shell. The calculations with the 6-31++G** basis set were done with Cartesian functions (6d).

The geometries optimized at the B3LYP/6-31++G** level were then used in single-point energy calculations at the second-order Møller–Plesset (MP2) level with different basis sets including the correlation-consistent basis sets denoted by aug-cc-pVXZ (X = D, T, and Q).[32–35] The calculations with the correlation consistent basis sets were done with spherical harmonic basis functions (5d, 7f, 9g). To extrapolate to the frozen core complete basis set (CBS) limit, we used a three-parameter, mixed exponential/Gaussian function of the form:

$$E(x) = E_{\text{CBS}} + B\exp[-(x-1)] + \text{C}\exp[-(x-1)^2] \quad (6)$$

where $x = 2$, 3, and 4 for aug-cc-pVDZ, aug-cc-pVTZ, and aug-cc-pVQZ, respectively.[34] Additional calculations at the coupled-cluster with single and double substitutions with a noniterative triples correction (CCSD(T))[36] level were also done with the correlation-consistent basis sets when possible as discussed below. We previously showed in our calculations[28] of $\Delta G^{298}_{\text{hyd}}(\text{H}^+)$ that we can ignore the corrections due to core–valence interactions and relativistic effects. The overall correction to the electronic energy change because of the core–valence correlation and scalar relativistic effects on $\Delta G^{298}_{\text{hyd}}(\text{H}^+)$ is less than 0.1 kcal/mol.[28]

Finally, we need to evaluate the bulk solvent shift, $\Delta\Delta G_{\text{sol}}[\text{HO}^-,n]$, by performing SCRF calculations on the supermolecular solutes $(\text{H}_2\text{O})_n$ and $\text{HO}^-(\text{H}_2\text{O})_n$. The reliability of the SCRF calculation results is dependent on the accuracy of the calculated solvent polarization potential (representing the long-range solute–solvent interaction) in addition to the accuracy of the quantum chemical approximation level for predicting the gas-phase results. Within the continuum model of solvation, the exact solvent electrostatic polarization potential corresponding to a given solute electronic wave function is determined by the solution of the requisite Poisson's equation under certain boundary condition.[25a,26] The full solvent electrostatic polarization consists of both surface and volume polarization.[25a] The latter is due to the part of the solute electron charge which quantum mechanically penetrates outside the cavity accommodating the solute. A surface and volume polarization for the electrostatic interaction (SVPE) procedure[25] has recently been developed to fully evaluate both the surface and volume polarization, and this procedure is also known as the fully polarizable continuum model (FPCM).[27,28,37,38] This SVPE procedure, implemented in a local version of the *GAMESS* program,[39] is currently the only implementation capable of directly determining the volume polarization for a general irregularly shaped solute cavity in addition to the more commonly treated surface polarization. In other SCRF implementations, volume polarization effects are ignored or approximately modeled by modifying the surface polarization charge distribution through a simulation and/or charge renormalization,[22a,26,40–42] or the solute charge distribution is simply represented by a set of point charges at the solute nuclei.[21,23] Because the solute cavity surface is defined as a solute electron charge isodensity contour determined self-consistently during the SVPE iteration process, the SVPE results, converged to the exact solution of Poisson's equation with a given numerical tolerance,[25a] depend only on the contour value at a given dielectric constant and on the quantum chemical approach that has been used. A single parameter value of 0.001 au has been determined based on an extensive calibration study[25c] using the experimental conformational free energy differences (62 experimental observations) of various polar solutes in various solvents. On the basis of the fitting process employed in the calibration, the root-mean-squares (rms) deviation of the 62 experimental values from the results calculated by SVPE method using the 0.001 au contour is 0.096 kcal/mol.[25c] The SVPE procedure using the 0.001 au contour has been shown to be reliable for evaluating the bulk solvent effects.[25c,27,28] It has also been shown that the solvent shifts determined by SVPE calculations are rather insensitive to the electron correlation level and basis set used, and it is sufficient to perform the SVPE calculations at the MP2/6-31++G** level as done for the calculation of the free energy of solvation of the proton.[28] Therefore, we evaluated $\Delta\Delta G_{\text{sol}}[\text{HO}^-,n]$ using the SVPE procedure at the MP2/6-31++G** level. We used a value of 78.5 for the dielectric constant of water.

The geometry optimizations were performed by using the *Gaussian 98* program,[43] and the SVPE solvation calculations were performed by using a local version of the *GAMESS* program[39] on a 16-processor SGI Origin 2000 computer. The other more time-consuming MP2 and CCSD(T) gas-phase energy calculations were performed by using the *NWChem* program[44] on a 512-processor IBM SP massively parallel supercomputer. The largest number of contracted basis functions (BFs) used in the MP2 energy calculations is 2190, whereas the largest number of contracted BFs used in the CCSD(T) calculations is 437.

Results and Discussion

Geometries. The optimized geometries of the various neutral and anionic clusters are shown in Figures 1–4. The most stable structure of the water tetramer, $(\text{H}_2\text{O})_4$, has been shown to be cyclic[21,22a] as depicted in Figure 1. Previous computational and experimental studies[45,46] have indicated that the most stable water octamer, $(\text{H}_2\text{O})_8$, exists in a cubic structure. Of six possible cubic isomers, the D_{2d} and S_4 symmetry structures (see Figure 1) have been calculated to be ~2 kcal/mol more strongly bound than the other four.[45f] The D_{2d} and S_4 symmetry structures each contain a total of 12 hydrogen bonds, four in each of two cyclic tetramer subunits and four bridging the two tetramers. The D_{2d} and S_4 structures are distinguished by having the hydrogen bonds

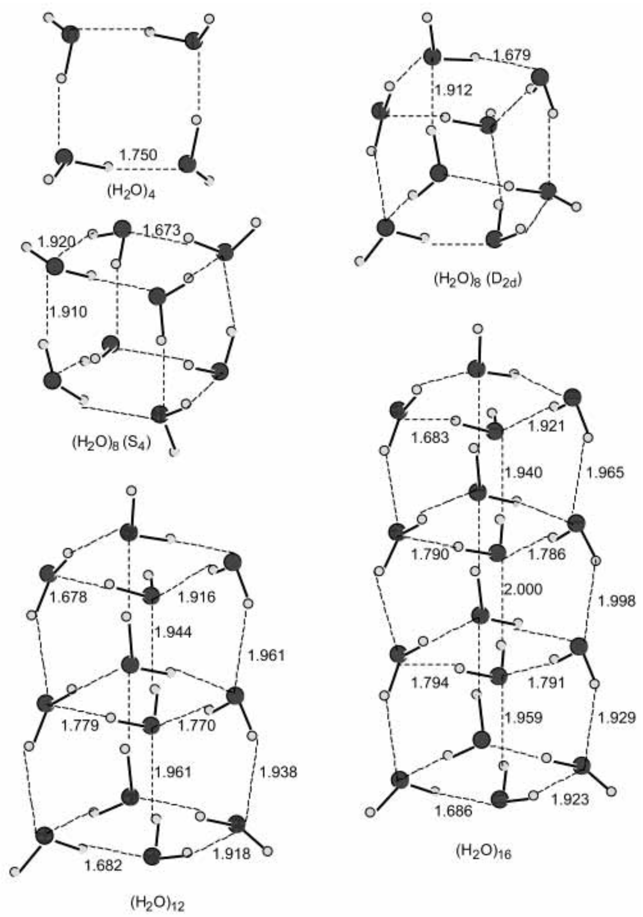

Figure 1. Geometries of water clusters, $(H_2O)_n$ ($n = 4$, 8, 12, and 16), optimized at the B3LYP/6-31++G** level. Independent key internuclear distances in Å for hydrogen bonds are indicated. Small spheres are hydrogens, and large spheres are oxygens.

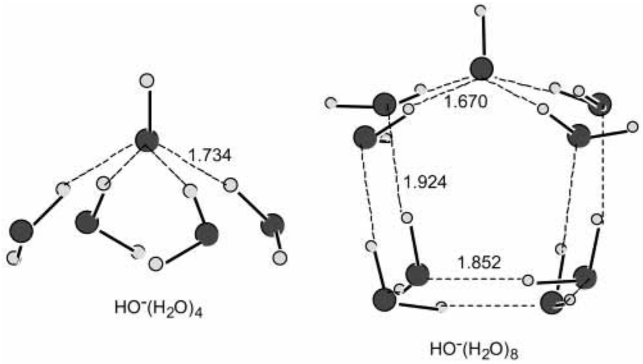

Figure 2. Geometries of the most stable $HO^-(H_2O)_4$ and $HO^-(H_2O)_8$ structures optimized at the B3LYP/6-31++G** level. Independent key internuclear distances in Å for hydrogen bonds are indicated. Small spheres are hydrogens, and large spheres are oxygens.

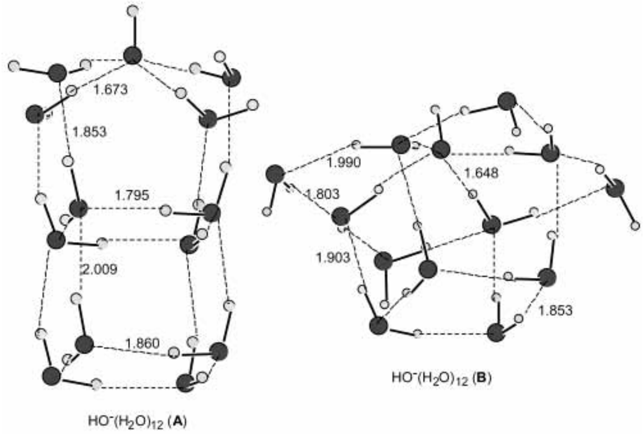

Figure 3. Geometries of two stable $HO^-(H_2O)_{12}$ structures optimized at the B3LYP/6-31++G** level. Independent key internuclear distances in Å for hydrogen bonds are indicated. Small spheres are hydrogens, and large spheres are oxygens.

within the tetramers oriented in the opposite (D_{2d}) or same (S_4) directions. It is, therefore, not surprising that the energies of the D_{2d} and S_4 structures were calculated to be nearly the same, although the electronic energy of the D_{2d} structure calculated at the MP2/aug-cc-pVDZ level using the geometry optimized with the TIP4P potential was estimated to be ∼0.1−0.2 kcal/mol lower than that of the S_4 structure calculated at the same level.[45f] We optimized the geometries of both the D_{2d} and S_4 structures at the B3LYP/6-31++G** level and found that further inclusion of the contributions of thermal and vibrational corrections in the Gibbs free energies significantly decreases the free energy difference. Our calculations at the B3LYP/6-31++G**//B3LYP/6-31++G**, MP2/6-31++G**//B3LYP/6-31++G**, MP2/aug-cc-pVDZ//B3LYP/6-31++G**, and MP2/aug-cc-pVTZ//B3LYP/6-31++G** levels all consistently suggest a negligible free energy difference (within 0.01 kcal/mol) between the D_{2d} and S_4 structures shown in Figure 1.

It has been shown that the lowest-energy structural forms of the larger clusters, including $(H_2O)_{12}$ and $(H_2O)_{16}$, have fused cubic structures based on using the cubic D_{2d}/S_4 structures as building blocks.[45f] The geometries of these cluster structures optimized at the B3LYP/6-31++G** level are also shown in Figure 1.

The first solvation shell structure of the hydroxide ion (HO^-) has been investigated extensively.[22a,47,48] It has been found that the maximum number of water molecules that can form hydrogen bonds with the oxygen atom in HO^- is five in the gas phase and that this structure is a local minimum.[48] However, calculations of the relative stability of all possible cluster structures of $HO^-(H_2O)_n$ for a given n show that the most stable structure of an $HO^-(H_2O)_n$ ($n \geq 4$) cluster has only four water molecules hydrogen-bonded to the HO^-.[47,48] Any additional water molecules beyond these four form water−water hydrogen bonds, instead of any additional hydroxide-water hydrogen bond, in the most stable structure. Thus, the first solvation shell of HO^- consists of four water molecules. Our optimized geometry of the most stable $HO^-(H_2O)_4$ structure has C_4 symmetry, as shown in Figure 2.

The second solvation shell contains eight water molecules having hydrogen bonds with the four first-solvation-shell water molecules. Thus, a description of the complete first and second solvation shells requires a minimum of 12 water molecules, forming the cluster $HO^-(H_2O)_{12}$ (**B**) shown in Figure 3. We also found another stable structure of $HO^-(H_2O)_{12}$, denoted by $HO^-(H_2O)_{12}$ (**A**) as shown in Figure 3. Both the $HO^-(H_2O)_{12}$ (**A**) and $HO^-(H_2O)_{12}$ (**B**) optimized structures have exactly the same number of hydrogen bonds and have C_4 symmetry. A remarkable structural difference between the two structures is that in $HO^-(H_2O)_{12}$ (**A**) only four water molecules exist in the second solvation shell and have hydrogen bonds with the first-solvation-shell water molecules. The other four water molecules exist in the third solvation shell and have hydrogen bonds with the second-solvation-shell water molecules. So, the $HO^-(H_2O)_{12}$ (**A**) structure has a complete first solvation shell and incomplete second and third solvation shells, whereas the $HO^-(H_2O)_{12}$ (**B**)

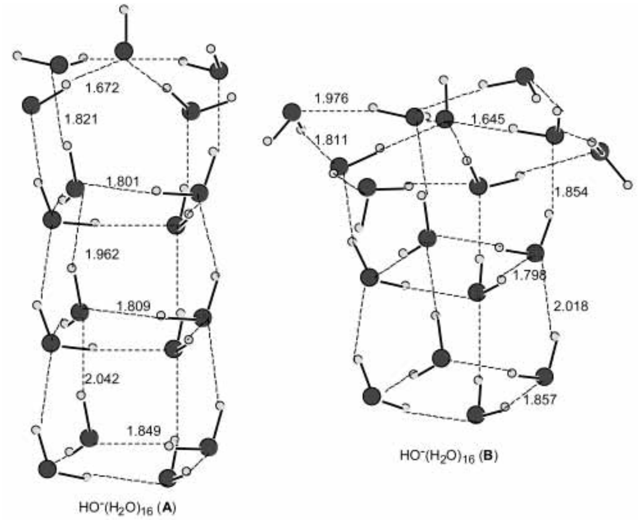

Figure 4. Geometries of two stable $HO^-(H_2O)_{16}$ structures optimized at the B3LYP/6-31++G** level. Independent key internuclear distances in Å for hydrogen bonds are indicated. Small spheres are hydrogens, and large spheres are oxygens.

structure includes the complete first and second solvation shells. The $HO^-(H_2O)_{12}$ (**A**) structure is lower in terms of the Gibbs free energy in the gas phase as compared to the $HO^-(H_2O)_{12}$ (**B**) structure by ~1 kcal/mol as calculated at the B3LYP/6-31++G**//B3LYP/6-31++G**, MP2/6-31++G**//B3LYP/6-31++G**, MP2/aug-cc-pVDZ//B3LYP/6-31++G**, and MP2/aug-cc-pVTZ//B3LYP/6-31++G** levels. This is most likely due to the much larger dipole moment along the C_4 axis of the water cluster stabilizing the HO^- in the **A** structure. The dipole moments of the water clusters, $(H_2O)_{12}$ (**A**) and $(H_2O)_{12}$ (**B**), constructed by removing the HO^- from $HO^-(H_2O)_{12}$ (**A**) and $HO^-(H_2O)_{12}$ (**B**) were calculated to be 19.5 and 4.4 D, respectively, at the B3LYP/6-31++G** level in support of this conclusion.

On the basis of the results obtained for $n = 12$, we note that the most stable structure of $HO^-(H_2O)_8$ (Figure 2) is the common building block of the $HO^-(H_2O)_{12}$ (**A**) and $HO^-(H_2O)_{12}$ (**B**) structures and contains the complete first solvation shell and an incomplete second solvation shell. The $HO^-(H_2O)_8$ structure also has C_4 symmetry.

Starting from the most stable structure, $HO^-(H_2O)_{12}$ (**A**), for $n = 12$, one could construct the lowest-energy structures of $HO^-(H_2O)_{16}$ according to two possible ways. The first way is to add the four water molecules to the fourth solvation shell to form hydrogen bonds with the third-solvation-shell water molecules as found for the neutral cluster. In this way, we obtained the structure for $HO^-(H_2O)_{16}$ (**A**) shown in Figure 4. The second way is to add the four water molecules so that they form hydrogen bonds with the first-solvation-shell water molecules to complete the second solvation shell just as in the structure of $HO^-(H_2O)_{12}$ (**B**) leading to the structure for $HO^-(H_2O)_{16}$ (**B**) shown in Figure 4. Both structures have C_4 symmetry. The optimized $HO^-(H_2O)_{16}$ (**A**) structure was calculated to be lower in terms of the Gibbs free energy in the gas phase as compared to the optimized $HO^-(H_2O)_{16}$ (**B**) structure by ~1 kcal/mol.

TABLE 1: Absolute Hydration Free Energy of the Hydroxide Ion (in kcal/mol) Calculated as the Free Energy Change from HO^-(gas) + $(H_2O)_n$(aq) to $HO^-(H_2O)_n$(aq) at $T = 298$ K

	Gibbs free energy change			
calculation method[a]	$n = 4$	$n = 8$	$n = 12$	$n = 16$
Without Bulk Solvent Shift (i.e., $\Delta G_{gas}[HO^-,n]$)[b]				
B3LYP/6-31++G**	−48.3	−59.8	−68.0	−71.6
MP2/6-31++G**	−49.3	−59.9	−68.0	−71.5
MP2/aug-cc-pVDZ	−48.1	−58.8	−67.0	−70.8
MP2/aug-cc-pVTZ	−47.9	−59.2	−67.3	
MP2/aug-cc-pVQZ	−47.5	−59.0	−67.1	
MP2/CBS	−47.3	−58.8	−66.9	
CCSD(T)/aug-cc-pVDZ	−49.6	−60.3		
CCSD(T)/aug-cc-pVTZ	−49.4			
best estimate	−48.8[d]	−60.3[d]	−68.4[d]	
bulk solvent shift (i.e. $\Delta\Delta G_{sol}[HO^-,n]$)[c]	−42.1	−41.1	−36.1	−32.6
Including Bulk Solvent Shift (i.e., $\Delta G_{hyd}[HO^-,n]$)				
B3LYP/6-31++G**	−90.4	−100.9	−104.1	−104.2
MP2/6-31++G**	−90.5	−101.0	−104.1	−104.2
MP2/aug-cc-pVDZ	−90.2	−99.9	−103.2	−103.4
MP2/aug-cc-pVTZ	−90.0	−100.3	−103.4	
MP2/aug-cc-pVQZ	−89.7	−100.1	−103.2	
MP2/CBS	−89.4	−99.9	−103.0	
CCSD(T)/aug-cc-pVDZ	−91.7	−101.4		
CCSD(T)/aug-cc-pVTZ	−91.5			
best estimate	−90.9	−101.4	−104.5	

[a] Computational method used for the gas-phase energy calculations. All energy calculations were performed by using the geometries optimized at the B3LYP/6-31++G** level. [b] Without bulk solvent effects, $\Delta G_{gas}[HO^-,n]$ is the free energy of reaction 1. [c] Calculated by using the SVPE approach at the MP2/6-31++G** level. [d] The best estimate is the MP2/CBS value plus the higher order electron correlation correction, −1.5 kcal/mol, as the energy difference between the MP2/aug-cc-pVDZ value and the CCSD(T)/aug-cc-pVDZ value or the MP2/aug-cc-pVTZ value and the CCSD(T)/aug-cc-pVTZ value for both $n = 4$ and 8.

Free Energies of Solvation. The energy results for $n = 4$, 8, 12, and 16 using the most stable geometries optimized at the B3LYP/6-31++G** level are summarized in Table 1. The convergence of the calculated hydration free energy with respect to n can be examined by comparing the results calculated at the same level of theory for different n values. As shown in Table 1, there is a large change, ~10 kcal/mol, in the calculated hydration free energy from $n = 4$ to 8. The change, ~3 kcal/mol, from $n = 8$ to 12 is smaller, but large enough that it cannot be ignored. The change in energies from $n = 12$ to 16 is negligible, ~0.1−0.2 kcal/mol based on the energy calculations at the B3LYP/6-31++G**, MP2/6-31++G**, and MP2/aug-cc-pVTZ levels. The convergence with respect to n does not depend much on the level of theory used for the gas phase calculations. Our results show that, to accurately determine the absolute free energy of hydration of the hydroxide ion, one must include in the supermolecule not only all solvent water molecules in the first solvation shell but also solvent molecules in the second and third solvation shells (in the axial direction). The convergence of the number of water molecules that must be explicitly included in the supermolecule calculations for the free energy of hydration for the hydroxide ion is significantly slower than that for the proton.[28] Only the first solvation shell of the hydronium ion (H_3O^+) must be treated quantum mechanically for the latter (a total of four water molecules with respect to the bare proton) as compared to 12 water molecules for the OH^- solvation energy calculations. This difference could be due to the much stronger solvent polarization in the axial direction needed to stabilize the diffuse negative charge on HO^- which is highly concentrated on the O atom. The negative charge on the O atom in HO^- is over −1.0 e, actually ~−1.21 e, as determined at the MP2/aug-cc-pVQZ level by fitting the electrostatic potential (ESP) at points selected according to the Merz−Singh−Kollman scheme.[49] The ESP charge on the hydroxide oxygen atom determined at the MP2/6-31++G**

level is −1.29 e in HO^- and −1.01 e in $HO^-(H_2O)_{12}$ (**A**). The corresponding ESP charge on the hydroxide hydrogen atom in $HO^-(H_2O)_{12}$ (**A**) was calculated as +0.33 e giving a net ESP charge for the hydroxide ion in $HO^-(H_2O)_{12}$ (**A**) of −0.68 e. Thus, the negative ESP charge on the hydroxide oxygen atom is significantly reduced (by −0.28 e) in $HO^-(H_2O)_{12}$ (**A**) as compared to that in the free ion, and there is a significant amount of electronic charge, −0.32 e, transferred to the solvent water molecules.

Because the hydration free energy calculations are well converged at $n = 12$ for hydroxide ion, we just need to perform high-level energy calculations on the aqueous clusters up to $n = 12$. The CCSD(T) method can predict total molecular dissociation energies involving covalent bonds based on the valence electrons to within tenths of a kcal/mol[51,52] when a sufficiently large basis set is used and extrapolated to the complete basis set (CBS) limit and if other effects such as core-valence correlation, relativity, and zero-point energies are properly accounted for. The MP2 method has been shown to give very good energies for hydrogen bonded systems.[53] We have neglected the core-valence correlation and relativistic effects based on our calculations on $\Delta G^{298}_{\mathrm{hyd}}(H^+)$,[28] which showed that the sum of these corrections is small. We can extrapolate the MP2 energies to the CBS limit by using the augmented correlation-consistent basis sets, aug-cc-pVDZ, aug-cc-pVTZ, and aug-cc-pVQZ. The extrapolated MP2/CBS results lead to $\Delta G_{\mathrm{hyd}}[HO^-,n] = -89.4$, -99.9, and -103.0 kcal/mol for $n = 4$, 8, and 12, respectively. We were unable to perform CCSD(T) energy calculations on the clusters with $n = 12$ using any of the augmented correlation-consistent basis sets, but we were able to carry out the CCSD(T) energy calculations for $n = 4$ with the aug-cc-pVDZ and aug-cc-pVTZ basis sets and for $n = 8$ with the aug-cc-pVDZ basis set. The three values for the free energy of hydration determined at the CCSD(T) level are ∼1.5 kcal/mol greater than the corresponding MP2 values with the same basis set and are not dependent on n. We then estimate the CCSD(T)/CBS value to be sum of the MP2/CBS value and the higher order electron correlation correction of 1.5 kcal/mol for all values of n. Thus, our best estimate of the absolute hydration free energy of hydroxide ion, $\Delta G^{298}_{\mathrm{hyd}}(HO^-)$, is −104.5 kcal/mol for the usually used standard state (i.e., the ideal gas phase and hypothetical 1 M solution without solute−solute interaction at $T = 298.15$ K and $P = 1$ atm as discussed previously[28]). Unless indicated otherwise, all hydration free energies discussed below are for these standard states.

Our predicted absolute hydroxide hydration free energy of −104.5 kcal/mol is ∼3.5 kcal/mol more positive than the −108.0 kcal/mol predicted by Pliego and Riveros[47b] but significantly more negative than the ∼−400 kJ/mol (∼−96 kcal/mol) predicted by Mejias and Lago.[22a] The value reported by Pliego and Riveros[47b] was determined by Monte Carlo simulation and free energy perturbation using classical model potentials. The calculations reported by Mejias and Lago[22a] were performed by using a conductor-like screening model (COSMO) and DFT. Ignoring the inherent accuracy of their DFT energy calculations in gas phase, their COSMO-DFT calculations significantly underestimated the bulk solvent effects. Their $\Delta G_{\mathrm{hyd}}[HO^-,n]$ calculations are apparently not converged. The largest and next largest numbers of water molecules considered in their work are 12 and 8. The change of their calculated $\Delta G_{\mathrm{hyd}}[HO^-,n]$ value from $n = 8$ to 12 is ∼−17 kcal/mol.[22a]

Comparison with Available Experimental Data. As noted in the Introduction, the "experimental" absolute hydration free energy of the hydroxide ion in the literature has a wide range from −90.6 to −110.0 kcal/mol.[22] Our predicted absolute hydroxide hydration free energy of −104.5 kcal/mol falls in this range and is closer to the lower end.

The $\Delta G^{298}_{\mathrm{hyd}}(HO^-)$ value of −104.5 kcal/mol predicted in this study combined with our previously predicted $\Delta G^{298}_{\mathrm{hyd}}(H^+)$ value of −262.4 kcal/mol[28] gives the sum of the absolute hydration free energies of the proton and hydroxide as −366.9 kcal/mol. This theoretical prediction can be compared with well-established experimental thermodynamic data.

There has been some inconsistency in the literature because of differences in the definition of the standard reference states for the absolute hydration free energies of different solutes. This inconsistency has led to rather different experimental values for the sum of the hydration free energies of the proton and hydroxide. For example, the experimental $\Delta G^{298}_{\mathrm{hyd}}(H^+) + \Delta G^{298}_{\mathrm{hyd}}(HO^-)$ value should be −351.1 kcal/mol for the standard states described above according to Table 5 in ref 22b, whereas a recent analysis reported by Tissandier et al.[20a] shows that the experimental $\Delta G^{298}_{\mathrm{hyd}}(H^+) + \Delta G^{298}_{\mathrm{hyd}}(HO^-)$ value should be −1535.3 kJ/mol (∼−366.95 kcal/mol) for the same standard states. Below we present a detailed analysis of the experimental thermodynamic data to ensure a consistent comparison between our theoretical prediction and well-established experiment data.

The experimental Gibbs free energy of the gas-phase reaction, $H_2O(g) \rightarrow H^+(g) + HO^-(g)$, at $T = 298.15$ K and $P = 1$ bar (∼ 1 atm) listed in the NIST Standard Reference Database[53] is $\Delta G^{298}[H_2O(g) \rightarrow H^+(g) + HO^-(g)] = 384.1 \pm 0.2$ kcal/mol. Very recently, this $\Delta G^{298}[H_2O(g) \rightarrow H^+(g) + HO^-(g)]$ value has been revised to 383.61 ± 0.07 kcal/mol, on the basis of a combination of new sophisticated experimental and computational results for the heat of formation of the OH radical which revises this value by almost 0.5 kcal/mol.[51b,54]

The NBS (now NIST) tables[55] provide the experimental Gibbs free energies of $H_2O(g)$ and H_2O(l, i.e. 55.5 M) leading to $\Delta G^{298}[H_2O(g) \rightarrow H_2O(\mathrm{l, i.e.\ 55.5\ M})] = -2.05$ kcal/mol at $T = 298.15$ K and $P = 1$ bar. It should be emphasized that the $\Delta G^{298}[H_2O(g) \rightarrow H_2O(\mathrm{l, i.e.\ 55.5\ M})]$ value of −2.05 kcal/mol must be distinguished from the usually used experimental hydration free energy of −6.32 kcal/mol for the water molecule.[56] The two values are associated with different standard state definitions and are consistent with each other. The experimental hydration free energy of −6.32 kcal/mol was determined as the free energy change from the hypothetical ideal gas with the same density as liquid water (i.e., 55.5 mol L^{-1}, instead of 1/24.5 mol L^{-1} corresponding to $P = 1$ atm) to liquid water. The contribution of the entropy change of the expansion process, $H_2O(\mathrm{gas,\ 55.5\ mol\ L^{-1}}) \rightarrow H_2O(\mathrm{gas,\ 1/24.5\ mol\ L^{-1}})$, to the free energy is −4.27 kcal/mol at $T = 298.15$ K.[56]

From the established experimental thermodynamic equilibration of water autoionization

$$\Delta G^{298}[H_2O(\mathrm{l,\ i.e.\ 55.5\ M}) \rightarrow H^+(10^{-7}\ \mathrm{M}) + HO^-(10^{-7}\ \mathrm{M})] = 0\ \mathrm{kcal/mol} \quad (7)$$

at $T = 298.15$ K and $P = 1$ atm. Therefore

$$\Delta G^{298}[H_2O(\mathrm{l,\ i.e.\ 55.5\ M}) \rightarrow H^+(1\ \mathrm{M}) + HO^-(1\ \mathrm{M})] = 19.09\ \mathrm{kcal/mol} \quad (8)$$

or

$$\Delta G^{298}[H_2O(\mathrm{hypothetical\ 1\ M}) \rightarrow H^+(1\ \mathrm{M}) + HO^-(1\ \mathrm{M})] = 21.47\ \mathrm{kcal/mol} \quad (9)$$

Considering the solvation shift of the free energy of the reaction $H_2O \rightarrow H^+ + HO^-$, we have

$$\Delta G^{298}_{\text{hyd}}(H^+) + \Delta G^{298}_{\text{hyd}}(HO^-) - \Delta G^{298}_{\text{hyd}}[H_2O(g) \rightarrow H_2O(l, \text{i.e. } 55.5\text{ M})] = \Delta G^{298}[H_2O(l, \text{i.e. } 55.5\text{ M}) \rightarrow H^+(1\text{ M}) + HO^-(1\text{ M})] - \Delta G^{298}[H_2O(g) \rightarrow H^+(g) + HO^-(g)] \quad (10)$$

Based on the very recently revised experimental $\Delta G^{298}[H_2O(g) \rightarrow H^+(g) + HO^-(g)]$ value of 383.61 ± 0.07 kcal/mol,[54] eqs 8 and 10 lead to

$$\Delta G^{298}_{\text{hyd}}(H^+) + \Delta G^{298}_{\text{hyd}}(HO^-) \approx -366.6 \pm 0.1\text{ kcal/mol} \quad (11a)$$

whereas using the NIST-listed $\Delta G^{298}[H_2O(g) \rightarrow H^+(g) + HO^-(g)]$ value of 384.1 ± 0.2 kcal/mol[53] gives

$$\Delta G^{298}_{\text{hyd}}(H^+) + \Delta G^{298}_{\text{hyd}}(HO^-) \approx -367.1 \pm 0.2\text{ kcal/mol} \quad (11b)$$

The experimental $\Delta G^{298}_{\text{hyd}}(H^+) + \Delta G^{298}_{\text{hyd}}(HO^-)$ value of -367.1 ± 0.2 kcal/mol based on the NIST database is consistent with the experimental value of -1535.3 kJ/mol (~ -366.95 kcal/mol ≈ -367.0 kcal/mol) listed by Tissandier et al.[20a] analyzing previously reported experimental thermodynamic data by a somewhat different path. Our predicted sum of the absolute hydration free energies of the proton and hydroxide, -366.9 kcal/mol, is slightly lower than the experimental value of -366.6 ± 0.1 kcal/mol based on the very recently revised gas phase experimental value, and slightly larger than the value of -367.1 ± 0.2 kcal/mol based on the NIST gas-phase experimental value for OH. The fact that the sum of the free energies of solvation for H^+ and HO^- agree so well with the well-established experimental value strongly supports the reliability of our calculated absolute hydroxide hydration free energy of -104.5 kcal/mol.

Conclusion

The absolute hydration free energy of the hydroxide ion, $\Delta G^{298}_{\text{hyd}}(HO^-)$, has been calculated to be -104.5 kcal/mol by using a reliable computational protocol of first-principles solvation-included electronic structure calculations, the same approach recently used to calculate the absolute hydration free energy of the proton. The sum of the $\Delta G^{298}_{\text{hyd}}(HO^-)$ value of -104.5 kcal/mol predicted in this study and our previously calculated $\Delta G^{298}_{\text{hyd}}(H^+)$ value of -262.4 kcal/mol gives a value of -366.9 kcal/mol, in excellent agreement with well-established experimental thermodynamic data. This excellent agreement suggests that the recently used supermolecule-continuum approach based on a recently developed surface and volume polarization for electrostatic interaction (SVPE; or fully polarizable continuum model (FPCM)) can also be used to predict reliable solvation energies for anions if enough solvent molecules are included in the supermolecule calculations. The supermolecule-continuum calculations on the hydroxide ion are much more computationally demanding than those on the proton because the convergence of the calculated results with respect to the number of explicitly included water molecules is slower for the hydroxide ion as compared to similar calculations for the proton.

Acknowledgment. This research was performed in the William R. Wiley Environmental Molecular Sciences Laboratory (EMSL), and part of the work was done using the Molecular Sciences Computing Facility (MSCF) in the EMSL at PNNL. The EMSL including the MSCF is a national user facility funded by the Office of Biological and Environmental Research of the U.S. Department of Energy. This work was supported in part by the U.S. Department of Energy, Office of Basic Energy Sciences, Geosciences Research Program, contract 18328. PNNL is a multiprogram national laboratory operated by Battelle Memorial Institute for the U.S. Department of Energy.

Supporting Information Available: Cartesian coordinates (in Å) of the lowest-energy geometries optimized at the B3LYP/6-31++G** level and the total energies (in au) with different methods for the optimized geometries. This material is available free of charge via the Internet at http://pubs.acs.org.

References and Notes

(1) Conway, B. E. *Ionic Hydration in Chemistry and Biophysics*; Elsevier: New York, 1981.

(2) Marcus, Y. *Ion Solvation*; Wiley: New York, 1985.

(3) Hille, B. *Ionic Channels of Excitable Membranes*, 2nd ed.; Sinauer: Sunderland, MA, 1992.

(4) Franks, N. P.; Lieb, W. R. *Nature* **1997**, *389*, 334.

(5) Gunshin, H.; Mackenzie, B.; Berger, U. V.; Gunshin, Y.; Romero, M. F.; Boron, W. F.; Nussberger, S.; Gollan, J. L.; Hediger, M. A. *Nature* **1997**, *388*, 482.

(6) Doyle, D. A.; Cabral, J. M.; Pfuetzner, R. A.; Kuo, A.; Gulbis, J. M.; Cohen, S. L.; Chait, B. T.; MacKinnon, R. *Science* **1998**, *280*, 69.

(7) MacKinnon, R.; Cohen, S. L.; Kuo, A.; Lee, A.; Chait, B. T. *Science* **1998**, *280*, 106.

(8) Nakamura, T.; Akutagawa, T.; Honda, K.; Underhill, A. E.; Coomber, A. T.; Friend, R. H. *Nature* **1998**, *394*, 159.

(9) Roux, B.; MacKinnon, R. *Science* **1999**, *285*, 100.

(10) Wu, K.; Iedema, M. J.; Cowin, J. P. *Science* **1999**, *286*, 2482.

(11) Anson, L. *Nature* **1999**, *402*, 739.

(12) MacFarlane, D. R.; Huang, J.; Forsyth, M. *Nature* **1999**, *402*, 792.

(13) Kolbe, M.; Besir, H.; Essen, L.-O.; Oesterhelt, D. *Science* **2000**, *288*, 1390.

(14) Weber, J. M.; Kelley, J. A.; Nielsen, S. B.; Ayotte, P.; Johnson, M. A. *Science* **2000**, *287*, 2461.

(15) Aqvist, J.; Luzhkov, V. *Nature* **2000**, *404*, 881.

(16) Williams, K. A. *Nature* **2000**, *403*, 112.

(17) Pasquarello, A.; Petri, I.; Salmon, P. S.; Parisel, O.; Car, R.; Tóth, É.; Powell, D. H.; Fischer, H. E.; Helm, L.; Merbach, A. *Science* **2001**, *291*, 856.

(18) Kielpinski, D.; Meyer, V.; Rowe, M. A.; Sackett, C. A.; Itano, W. M.; Monroe, C.; Wineland, D. J. *Science* **2001**, *291*, 1013.

(19) Kropman, M. F.; Bakker, H. J. *Science* **2001**, *291*, 2118.

(20) (a) Tissandier, M. D.; Cowen, K. A.; Feng, W. Y.; Gundlach, E.; Cohen, M. H.; Earhart, A. D.; Coe, J. V. *J. Phys. Chem. A* **1998**, *102*, 7787. (b) Klots, C. E. *J. Phys. Chem.* **1981**, *85*, 3585.

(21) Tawa, G. J.; Topol, I. A.; Burt, S. K.; Caldwell, R. A.; Rashin, A. A. *J. Chem. Phys.* **1998**, *109*, 4852.

(22) (a) Mejias, J. A.; Lago, S. *J. Chem. Phys.* **2000**, *113*, 7306. (b) Friedman, H. L.; Krishnan, V. V. *Water: A comprehensive treatise*; Plenum: New York, 1973. (c) Zhu, T.; Li, J.; Hawkins, G. D.; Cramer, C. J.; Truhlar, D. G. *J. Chem. Phys.* **1998**, *109*, 9177.

(23) Topol, I. A.; Tawa, G. J.; Burt, S. K.; Rashin, A. A. *J. Chem. Phys.* **1999**, *111*, 10998.

(24) Bandyopadhyay, P.; Gordon, M. S. *J. Chem. Phys.* **2000**, *113*, 1104.

(25) (a) Zhan, C.-G.; Bentley, J.; Chipman, D. M. *J. Chem. Phys.* **1998**, *108*, 177. (b) Zhan, C.-G.; Chipman, D. M. *J. Chem. Phys.* **1998**, *109*, 10543. (c) Zhan, C.-G.; Chipman, D. M. *J. Chem. Phys.* **1999**, *110*, 1611. (d) Zhan, C.-G.; Landry, D. W.; Ornstein, R. L. *J. Phys. Chem. A* **2000**, *104*, 7672.

(26) (a) Tomasi, J.; Persico, M. *Chem. Rev.* **1994**, *94*, 2027. (b) Cramer, C. J.; Truhlar, D. G. In *Solvent Effects and Chemical Reactions*; Tapia, O., Bertran, J., Eds.; Kluwer: Dordrecht, The Netherlands, 1996; p 1. (c) Chipman, D. M. *J. Chem. Phys.* **1997**, *106*, 10194. (d) Cramer, C. J.; Truhlar, D. G. *Chem. Rev.* **1999**, *99*, 2161. (e) Chipman, D. M. *J. Chem. Phys.* **2000**, *112*, 5558.

(27) Zhan, C.-G.; Landry, D. W.; Ornstein, R. L. *J. Am. Chem. Soc.* **2000**, *122*, 2621.

(28) Zhan, C.-G.; Dixon, D. A. *J. Phys. Chem. A* **2001**, *105*, 11534.

(29) (a) Becke, A. D. *J. Chem. Phys.* **1993**, *98*, 5648. (b) Lee, C.; Yang, W.; Parr, R. G. *Phys. Rev. B* **1988**, *37*, 785. (c) Stephens, P. J.; Devlin, F. J.; Chabalowski, C. F.; Frisch, M. J. *J. Phys. Chem.* **1994**, *98*, 11623.

(30) Hehre, W. J.; Radom, L.; Schleyer, P. v. R.; Pople, J. A. *Ab Initio Molecular Orbital Theory*; John Wiley & Sons: New York, 1987.

(31) The vibrational contributions to the entropies and the thermal energy corrections were calculated in the harmonic approximation. Anharmonic corrections will approximately cancel as there are comparable numbers of low-frequency modes: 10 frequencies for $(H_2O)_4$, 10 frequencies for $HO^-(H_2O)_4$, 22 frequencies for $(H_2O)_8$, 24 frequencies for $HO^-(H_2O)_8$, 33 frequencies for $(H_2O)_{12}$, 36 frequencies for $HO^-(H_2O)_{12}$, 46 frequencies for $(H_2O)_{16}$, and 48 frequencies for $HO^-(H_2O)_{16}$ below 1 kcal/mol $\sim$ 350 cm^{-1} where $kT \sim 0.6$ kcal/mol = 210 cm^{-1}.

(32) Dunning, T. H., Jr. *J. Chem. Phys.* **1989**, *90*, 1007.

(33) Kendall, R. A.; Dunning, T. H., Jr.; Harrison, R. J. *J. Chem. Phys.* **1992**, *96*, 6796.

(34) Peterson, K. A.; Wood, D. E.; Dunning, T. H., Jr. *J. Chem. Phys.* **1994**, *100*, 7410.

(35) Woon, D. E.; Dunning, T. H., Jr. *J. Chem. Phys.* **1995**, *103*, 4572.

(36) (a) Purvis, G. D., III; Bartlett, R. J. *J. Chem. Phys*. **1982**, *76*, 1910. (b) Raghavachari, K.; Trucks, G. W.; Pople, J. A.; Head-Gordon, M. *Chem. Phys. Lett*. **1989**, *157*, 479. (c) Watts, J. D.; Gauss, J.; Bartlett, R. J. *J. Chem. Phys*. **1993**, *98*, 8718.

(37) Zhan, C.-G.; Norberto de Souza, O.; Rittenhouse, R.; Ornstein, R. L. *J. Am. Chem. Soc.* **1999**, *121*, 7279.

(38) (a) Zhan, C.-G.; Zheng, F. *J. Am. Chem. Soc.* **2001**, *123*, 2835. (b) Zhan, C.-G.; Niu, S.; Ornstein, R. L. *J. Chem. Soc., Perkin Trans. 2* **2001**, *1*, 23. (c) Zhan, C.-G.; Landry, D. W. *J. Phys. Chem. A* **2001**, *105*, 1296.

(39) Schmidt, M. W.; Baldridge, K. K.; Boatz, J. A.; Elbert, S. T.; Gordon, M. S.; Jensen, J. H.; Koseki, S.; Matsunaga, N.; Nguyen, K. A.; Su, S. J.; Windus, T. L.; Dupuis, M.; Montgomery, J. A. *J. Comput. Chem.* **1993**, *14*, 1347.

(40) Barone, V.; Cossi, M.; Tomasi, J. *J. Chem. Phys.* **1997**, *107*, 3210.

(41) Tomasi, J.; Mennucci, B.; Cances, E. *J. Mol. Struct. (THEOCHEM)* **1999**, *464*, 211.

(42) (a) Cancès, E.; Mennucci, B. *J. Chem. Phys.* **2001**, *114*, 4744. (b) Cossi, M.; Rega, N.; Scalmani, G.; Barone, V. *J. Chem. Phys.* **2001**, *114*, 5691.

(43) Frisch, M. J.; Trucks, G. W.; Schlegel, H. B.; Scuseria, G. E.; Robb, M. A.; Cheeseman, J. R.; Zakrzewski, V. G.; Montgomery, J. A., Jr.; Stratmann, R. E.; Burant, J. C.; Dapprich, S.; Millam, J. M.; Daniels, A. D.; Kudin, K. N.; Strain, M. C.; Farkas, O.; Tomasi, J.; Barone, V.; Cossi, M.; Cammi, R.; Mennucci, B.; Pomelli, C.; Adamo, C.; Clifford, S.; Ochterski, J.; Petersson, G. A.; Ayala, P. Y.; Cui, Q.; Morokuma, K.; Malick, D. K.; Rabuck, A. D.; Raghavachari, K.; Foresman, J. B.; Cioslowski, J.; Ortiz, J. V.; Stefanov, B. B.; Liu, G.; Liashenko, A.; Piskorz, P.; Komaromi, I.; Gomperts, R.; Martin, R. L.; Fox, D. J.; Keith, T.; Al-Laham, M. A.; Peng, C. Y.; Nanayakkara, A.; Gonzalez, C.; Challacombe, M.; Gill, P. M. W.; Johnson, B. G.; Chen, W.; Wong, M. W.; Andres, J. L.; Head-Gordon, M.; Replogle, E. S.; Pople, J. A. *Gaussian 98*, revision A.6; Gaussian, Inc.: Pittsburgh, PA, 1998.

(44) Anchell, J.; Apra, E.; Bernholdt, D.; Borowski, P.; Bylaska, E.; Clark, T.; Clerc, D.; Dachsel, H.; de Jong, W. A.; Deegan, M.; Dupuis, M.; Dyall, K.; Elwood, D.; Fann, G.; Fruchtl, H.; Glendenning, E.; Gutowski, M.; Harrison, R.; Hess, A.; Jaffe, J.; Johnson, B.; Ju, J.; Kendall, R.; Kobayashi, R.; Kutteh, R.; Lin, Z.; Littlefield, R.; Long, X.; Meng, B.; Nichols, J.; Nieplocha, J.; Rendall, A.; Rosing, M.; Sandrone, G.; Stave, M.; Straatsma, T.; Taylor, H.; Thomas, G.; van Lenthe, J.; Windus, T.; Wolinski, K.; Wong, A.; Zhang, Z. *NWChem*, version 4.0.1; Pacific Northwest National Laboratory: Richland, Washington, 2001.

(45) (a) Brink, G.; Glasser, L. *J. Phys. Chem.* **1984**, *88*, 3412. (b) Kim, K. S.; Dupuis, M.; Lie, G. C.; Clementi, E. *Chem. Phys. Lett.* **1986**, *131*, 451. (c) Tsai, C. J.; Jordan, K. D. *J. Chem. Phys.* **1991**, *95*, 3850. (d) Knochenmuss, R.; Leutwyler, S. *J. Chem. Phys.* **1992**, *96*, 5233. (e) Wales, D. J.; Ohmine, I. *J. Chem. Phys.* **1993**, *98*, 7245. (f) Tsai, C. J.; Jordan, K. D. *J. Phys. Chem.* **1993**, *97*, 5208. (g) Lee, C.; Chen, H.; Fitzgerald, G. *J. Chem. Phys.* **1995**, *102*, 1266. (h) Estrin, D. A.; Paglieri, L.; Corongui, G.; Clementi, E. *J. Phys. Chem.* **1996**, *100*, 8701.

(46) Gruenloh, C. J.; Carney, J. R.; Arrington, C. A.; Zwier, T. S.; Fredericks, S. Y.; Jordan, K. D. *Science* **1997**, *276*, 1678.

(47) (a) Novoa, J. J.; Mota, F.; del Valle, C. P.; Planas, M. *J. Phys. Chem. A* **1997**, *101*, 7842. (b) Pliego, J. R., Jr.; Riveros, J. M. *J. Chem. Phys.* **2000**, *112*, 4045. (c) Wei, D.; Proynov, E. I.; Milet, A.; Salahub, D. R. *J. Phys. Chem. A* **2000**, *104*, 2384.

(48) Masamura, M. *J. Comput. Chem.* **2001**, *22*, 31.

(49) (a) Besler, B. H.; Merz, K. M., Jr.; Kollman, P. A. *J. Comput. Chem.* **1990**, *11*, 431. (b) Singh, U. C.; Kollman, P. A. *J. Comput. Chem.* **1984**, *5*, 129.

(50) Peterson, K. A.; Xantheas, S. S.; Dixon, D. A.; Dunning, T. H., Jr. *J. Phys. Chem. A* **1998**, *102*, 2449.

(51) (a) Feller, D.; Peterson, K. A. *J. Chem. Phys.* **1999**, *110*, 8384. (b) Ruscic, B.; Feller, D.; Dixon, D. A.; Peterson, K. A.; Harding, L. B.; Asher, R. L.; Wagner, A. F. *J. Phys. Chem. A*, **2001**, *105*, 1.

(52) (a) Feller, D. *J. Chem. Phys.* **1992**, *96*, 6104. (b) Feyereisen, M. W.; Feller, D.; Dixon, D. A. *J. Phys. Chem*. **1996**, *100*, 2993. (c) Xantheas, S. *J. Chem. Phys.* **1996**, *104*, 8221.

(53) Mallard, W. G.; Linstrom, P. J., Eds., NIST Chemistry WebBook, NIST Standard Reference Database Number 69, February 2000, National Institute of Standards and Technology: Gaithersburg, MD, 2000 (http://webbook.nist.gov); Chase, M. W., Jr. *NIST-JANAF Thermochemical Tables*, 4th edition, *J. Phys. Chem. Ref. Data, Monograph 9*, **1998**.

(54) Ruscic, B.; Wagner, A. F.; Harding, L. B.; Asher, R. L.; Feller, D.; Dixon, D. A.; Peterson, K. A.; Song, Y.; Qian, X.; Ng, C.-Y.; Liu, J.; Chen, W.; Schwenke, D. W. *J. Phys. Chem. A* **2002**, *106*, 2727.

(55) Wagman, D. D.; Evans, W. H.; Parker, V. B.; Schumm, R. H.; Halow, I.; Bailey, S. M.; Churney, K. L.; Nutall, R. L. *J. Phys. Chem. Ref. Data* **1982**, *11*, Supplement No. 2.

(56) Ben-Naim, A.; Marcus, Y. *J. Chem. Phys.* **1984**, *81*, 2016.